Molecular Biology of the Cell
Vol. 12, 73–83, January 2001

The Catastrophe-promoting Activity of Ectopic Op18/Stathmin Is Required for Disruption of Mitotic Spindles But Not Interphase Microtubules

Per Holmfeldt,*§ Niklas Larsson,*§ Bo Segerman,* Bonnie Howell,†‡ Justin Morabito,† Lynne Cassimeris,† and Martin Gullberg*¶

*Department of Cell and Molecular Biology, Umeå University, S-901 87 Umeå, Sweden; and
†Department of Biological Sciences, Lehigh University, Bethlehem, Pennsylvania 18015

Submitted July 10, 2000; Revised October 6, 2000; Accepted October 27, 2000
Monitoring Editor: J. Richard McIntosh

Oncoprotein18/stathmin (Op18) is a microtubule (MT) destabilizing protein that is inactivated during mitosis by phosphorylation at four Ser-residues. Op18 has at least two functions; the N-terminal region is required for catastrophe-promotion (i.e., transition from elongation to shortening), while the C-terminal region is required to inhibit MT-polymerization rate in vitro. We show here that a "pseudophosphorylation" derivative of Op18 (i.e., four Ser- to Glu-substitutions at phosphorylation sites) exhibits a selective loss of catastrophe-promoting activity. This is contrasted to authentic phosphorylation, which efficiently attenuates all activities except tubulin binding. In intact cells, overexpression of pseudophosphorylated Op18, which is not phosphorylated by endogenous kinases, is shown to destabilize interphase MTs but to leave spindle formation untouched. To test if the mitotic spindle is sensitive only to the catastrophe-promoting activity of Op18 and resistant to C-terminally associated activities, N- and C-terminal truncations with defined activity-profiles were employed. The cell-cycle phenotypes of nonphosphorylatable mutants (i.e., four Ser- to Ala-substitutions) of these truncation derivatives demonstrated that catastrophe promotion is required for interference with the mitotic spindle, while the C-terminally associated activities are sufficient to destabilize interphase MTs. These results demonstrate that specific Op18 derivatives with defined activity-profiles can be used as probes to distinguish interphase and mitotic MTs.

INTRODUCTION

Microtubules (MTs) are polar polymers of α/β-tubulin heterodimers, which continuously switch between polymerization and depolymerization, a process termed "dynamic instability" (Desai and Mitchison, 1997). Regulation of dynamics is achieved by two broad classes of proteins, namely MT stabilizers and destabilizers. The former class is exemplified by microtubule-associated proteins (MAPs), which are, in general, thought to stabilize MTs by binding along the polymer (Cassimeris, 1999). Oncoprotein18/stathmin (Op18) and XKCM1 are two recently identified destabilizers of MTs, both of which bind free tubulin dimers. These two MT-destabilizing proteins have been shown to stimulate transitions from elongation to shortening of MTs and are referred to as catastrophe-promoters (Walczak, 2000).

Op18 is a 149-amino acid protein that was initially studied due to up-regulated expression in various types of malignancies and to a complex phosphorylation pattern that changes in response to multiple signals and through the cell cycle (Lawler, 1998). Phosphorylation, which switches off the MT-destabilizing function of Op18, is mediated by both cell cycle and cell surface receptor-regulated kinase systems on four Ser-residues (Deacon *et al.*, 1999). The phenotype of Op18 mutants that are deficient in kinase target sites in

‡ Present address: Dept. of Biology, University of North Carolina, Chapel Hill, NC 27599.
§ These authors contributed equally to this work and are listed in alphabetical order
¶ Corresponding author. E-mail address: Martin.Gullberg@cmb.umu.se.

Abbreviations used: AMP-PNP, adenyl-5′-yl imidodiphosphate; MT, microtubule; MAP, microtubule-associated protein; Op18, Oncoprotein 18/stathmin; Op18-F, FLAG epitope-tagged Op18; SDS-PAGE, sodium dodecyl sulfate-polyacrylamide gel electrophoresis; Op18-Δ4–24-tetraA-F, nonphosphorylatable Op18-F with amino acids 4–24 deleted and substituted at Ser- 3, 25, 38 and 63 with Ala; Op18-Δ100–147-tetraA-F, nonphosphorylatable Op18-F with amino acids 100–147 deleted and substituted at Ser-16, 25, 38 and 63 with Ala; Op18-tetraA, nonphosphorylatable full-length Op18 substituted at Ser-16, 25, 38 and 63 with Ala; Op18-tetraE, nonphosphorylatable full-length Op18 substituted at Ser-16, 25, 38 and 63 with Glu.

human cell lines reveal that phosphorylation-inactivation is essential to allow microtubules to segregate condensed chromosomes (Marklund *et al.*, 1994, 1996; Larsson *et al.*, 1995). Functional inactivation by extensive mitotic phosphorylation argues against an active role of Op18 during mitosis (Larsson *et al.*, 1997). Rather, signal-dependent control of Op18 activities via phosphorylation by several receptor regulated kinase systems suggests that the primary role for Op18 is to regulate the MT system in interphase cells (Gradin *et al.*, 1997, 1998). The physiological importance of such a role is indicated by the observation that ablation of the Op18 protein in interphase newt lung cells results in a 2.5-fold increase in MT polymer and an associated decrease in catastrophe frequency (Howell *et al.*, 1999a).

Op18 is the prototype member of a family of proteins with microtubule-regulatory function (Ozon *et al.*, 1997). Three major models have been proposed for regulation of microtubule dynamics mediated by Op18. The first and simplest of these models infers that Op18 acts as a pure tubulin-sequestering protein (Curmi *et al.*, 1997; Jourdain *et al.*, 1997). The second model infers that Op18 specifically promotes catastrophes (Belmont and Mitchison, 1996). The third model, which is an extension of the second model, infers that Op18 mediates at least two distinct activities—namely, catastrophe-promotion, which requires the N-terminal part of Op18, and a tubulin sequestering-like activity observed during MT-assembly in vitro, which requires the C-terminal part of Op18 (Howell *et al.*, 1999b; Larsson *et al.*, 1999b). The evidence for the third model includes genetic dissection of specific MT-directed activities both in intact cells and in vitro.

Specific combinations of Op18 phosphorylation on four Ser-residues attenuate the inhibitory activity of Op18 on taxol-driven MT polymerization in vitro (Larsson *et al.*, 1997) and the MT-destabilizing activity of overexpressed Op18 in intact cells (Gradin *et al.*, 1997, 1998). Substitution of Ser/Thr phosphorylation sites with negatively charged amino acids, such as Glu or Asp, results in at least a partial mimic of phosphorylation ("pseudophosphorylation"). However, apparently contradictory results have been reported using pseudophosphorylated mutants that have variously been shown to be completely inactive or to be undistinguishable from wild-type Op18 (Curmi *et al.*, 1997; Horwitz *et al.*, 1997; Larsson *et al.*, 1997; Gavet *et al.*, 1998). In these studies, diverse experimental systems in intact cells and in vitro have been employed to assess different activities of Op18. Because Op18 appears to mediate multiple MT/tubulin directed activities, conflicting results with pseudophosphorylation mutants may reflect selective attenuation of a specific activity of Op18.

Here we extend our mutant dissection of the molecular mechanisms by which Op18 regulates the MT-system. By analyzing MT/tubulin directed activities of a pseudophosphorylated Op18 derivative and specific N- and C-terminal truncation mutants of Op18, we provide evidence that interphase and mitotic MTs are differentially sensitive to specific activities of Op18.

MATERIALS AND METHODS

DNA constructs, expression and purification of recombinant proteins

Full-length Op18 with all 4 Ser-phosphorylation sites, namely Ser-16, Ser-25, Ser-38 and Ser-63, exchanged to Ala (Op18-tetraA) or Glu (Op18-tetraE) have been described (Larsson *et al.*, 1995, 1999a). Where indicated (-F), an 8-amino acid C-terminal Flag epitope was introduced as described (Marklund *et al.*, 1994). Flag-tagged truncated Op18 derivatives with deletions of either the sequence encoding amino acid 100–147 (Op18-Δ100–147-F) or the sequence encoding amino acid 4–24 (Op18-Δ4–24-F) have previously been described (Howell *et al.*, 1999b). It should be noted that Op18-Δ4–24-F was termed Op18-Δ5–25-F in its original description, but these derivatives are identical, as both positions 5 and 25 of Op18 contain Ser-residues. To construct nonphosphorylatable derivatives of Op18-Δ100–147-F and Op18-Δ4–24-F, four Ala substitutions were introduced by a general strategy, whereby mutations were introduced into subfragments of the coding region by single or overlapping polymerase chain reaction (Ho *et al.*, 1989). The resulting derivatives were termed Op18-Δ100–147-tetraA-F, which carries Ser-16, -25, -38, and -63 to Ala substitutions, and Op18-Δ4–24-tetraA-F, which carries Ser-25, -38, and -63 to Ala substitutions and an additional Ala substitution at the position Ser-3 to exclude phosphorylation of this residue in the amino acid 4–24 truncated protein. For expression of Op18 deletion mutants in human cell lines, coding regions were cloned, as *Hin*dIII to *Bam*HI fragments, into the corresponding sites of the Epstein-Barr Virus-based shuttle vector pMEP4 (Marklund *et al.*, 1994). Op18 derivatives were expressed and purified from *Escherichia coli* using pET-3d expression, as previously described (Marklund *et al.*, 1994). The coding sequence of fragments generated by polymerase chain reaction were confirmed by nucleotide sequence analysis using ABI PRISM dye terminator cycle sequencing kit from Perkin Elmer-Cetus (Norwalk, CT).

Quantification of Ectopic Op18 and Analysis of Op18 Phosphoisomers

To analyze Op18 phosphoisomers, we employed a native-PAGE system that separates Op18 according to the charge differences introduced by each of the four identified phosphorylations (Marklund *et al.*, 1993). Op18 phosphoisomers were detected by probing filters with affinity-purified anti-Op18 (Brattsand *et al.*, 1993). In experiments involving detection of truncated Op18 derivatives, which all contain a C-terminal Flag epitope, the anti-Flag-M2 antibody (Sigma, St. Louis, MO) together with the ECL detection system (Amersham Pharmacia Biotech, Arlington Heights, IL) were used. To determine Op18 expression levels, cell extracts were separated by SDS-PAGE together with graded amounts of recombinant Op18, as described (Marklund *et al.*, 1996).

Transfection of Human K562 Erythroleukemia Cells

The conditions used for transfection studies and the pMEP4 shuttle vector system have previously been described (Marklund *et al.*, 1994). Conditional expression of various Op18 derivatives was achieved by employing the hMTIIa promoter, which can be suppressed by low concentrations of EDTA (50 μM) and induced by Cd^{2+} (Marklund *et al.*, 1994). Using pMEP-Op18 derivatives without the Flag-epitope, 12 μg DNA was used for transfection, and expression was induced with 0.05 μM Cd^{2+}. To obtain comparable expression of Flag-epitope tagged full-length and truncated Op18 mutants, 0.5 μM Cd^{2+} was used to induce expression, and the amount of pMEP DNA was adjusted as follows: Op18-tetra-A-F, 6 μg; Op18-Δ4–24-tetraA-F, 6 μg; Op18-Δ100–147-tetraA-F, 12 μg. The total amount of DNA was adjusted to 12 μg by adding pMEP vector control.

Analysis of MT-Polymerization Status, Flow Cytometric Analysis, and Immunofluorescence

The cellular content of MT polymers was determined essentially as described (Gradin *et al.*, 1998). In brief, cells were resuspended in an MT-stabilizing buffer containing 0.05% saponin, to extract soluble tubulin, and were subsequently fixed in 4% paraformaldehyde/

0.05% glutaraldehyde. The remaining polymerized tubulin was stained with anti-α-tubulin (clone B-5–1-2, Sigma) and fluorescein-conjugated rabbit anti-mouse immunoglobulin. Fluorescence was quantitated by flow cytometry using a FACS-calibur together with the Cell Quest software (Becton-Dickinson, Mountain View, CA). To allow calculation of the percentage of polymerized tubulin in relation to the total amount of cellular tubulin, polymerization status in vector-control transfected cells was determined by quantitative western blotting (mean of 3 independent determinations: 58, ±12%). Relative fluorescence intensities of extracted cells were normalized in each experiment, assuming that the level in vector-control cells corresponded to 58% polymerized tubulin. This procedure faithfully reproduced the results obtained by quantification of soluble and particulate tubulin by western-blot analysis (Larsson *et al.*, 1999b), but with increased reproducibility. Within the time limits of the experiments, ectopic Op18 does not alter the cellular levels of total tubulin in K562 cells. Analysis of DNA content and quantification of mitotic cells, using the MPM-2 antibody, was performed by flow cytometric analysis as described (Marklund *et al.*, 1996). Immunofluorescence analysis and laser scanning confocal microscopy was performed as described (Marklund *et al.*, 1996).

Analysis of Op18-Tubulin Binding and Dissociation

A detailed account of Op18-tubulin equilibrium binding experiments has previously been reported (Larsson *et al.*, 1999b). In brief, C-terminally Flag-tagged Op18 derivatives (2 μM) and tubulin (0.8–36 μM) were mixed in PEM buffer (80 mM piperazine-*N*,*N*′-bis[2-ethanesulfonic acid], 1 mM EGTA, 4 mM Mg^{2+}, pH 7.5) and were allowed to associate on ice for ~ 15 min. Op18-F-tubulin mixes (48 μl) were added to agarose beads (12 μl), coupled with the Flag-epitope specific M2 antibody (Sigma), and incubated for 15 min at 8°C to capture Op18-F-tubulin complexes. To allow rapid separation of Op18-tubulin complexes bound to M2-beads, the bead suspension was applied into the cap of an 1.5 ml Eppendorf tube containing a bottom layer of 0.4 ml of PEM complemented with 27% sucrose/17% glycerol, pH 6.8, and a top layer of 0.2 ml of PEM with 17% glycerol, pH 6.8. The samples were centrifuged (1 min, 21 000 × *g*) to separate bead-bound and free material. To allow simultaneous quantification of Op18 and tubulin in the same sample, tubulin was labeled with [α-^{32}P]GTP and Op18 was labeled with [^{125}I]. There are two major benefits with this strategy. First, the amount of Op18-F (~ 30% of total Op18-F) present in the fraction of free tubulin after separation of M2 coupled beads can be compensated for in each data point; second, only biologically active (i.e. GTP-bound) tubulin was detected in the fraction of free tubulin. To calculate equilibrium dissociation constants, data points from equilibrium binding experiments were fitted either to a hyperbola or to a model assuming two-site positive cooperativity in binding (Koshland Jr *et al.*, 1966) as described (Larsson *et al.*, 1999b).

Dissociation rates of Op18-tubulin complexes were determined as described (Larsson *et al.*, 1999b). In brief, M2-beads coated with Flag-tagged Op18 derivatives were incubated with tubulin (20 μM) for 15 min at 8°C to attain equilibrium binding. Before centrifugation through a sucrose/glycerol cushion, bead suspensions were diluted 100-fold in PEM (pH 6.8 or pH 7.5) and incubated for 20 to 900 s. Op18-tubulin complexes were quantitated by the dual isotope labeling strategy described above. Dissociation rates were calculated assuming one phase exponential decay using GraphPad Prism software (San Diego, CA).

In Vitro Phosphorylation of Op18

Purified recombinant Op18 was in vitro phosphorylated on Ser-16 and Ser-63 to high stoichiometry with cAMP dependent protein kinase (New England BioLabs, Inc., Beverly, MA) by incubating 2.8 U kinase/μg Op18 in 50 mM Tris-HCl, pH 7.5, 10 mM $MgCl_2$, and 500 μM ATP for 3 h at 30°C. Reactions were terminated by heating to 75°C for 10 min and precipitated overnight at −20°C with 6 volumes of MeOH containing 1% sucrose. The precipitate was washed twice with 75% MeOH containing 1% sucrose, dried under vacuum, and resuspended in PEM buffer. To remove the protein kinase, which remained insoluble after MeOH precipitation, the final preparation of phosphorylated Op18 was clarified by centrifugation (15 min, 21,000X*g*). As controls, in vitro phosphorylations were also performed in the absence of ATP. Analysis of phosphorylated Op18 on native gels showed that more than 90% was phosphorylated on two sites, which have been identified as Ser-16 and Ser-63 in a previous study (Gradin *et al.*, 1998).

Assays of Tubulin GTPase Activity

Analysis of tubulin GTPase activity was performed in PEM buffer containing 5 mM adenyl-5′-yl imidodiphosphate (AMP-PNP; to inhibit nonspecific ATPase activity), as described (Larsson *et al.*, 1999b). In brief, tubulin was incubated with [α-^{32}P]GTP, tubulin-[α-^{32}P]GTP complexes were recovered by centrifugation through a desalting column (P-30 Micro Bio-Spin, Bio-Rad, Richmond, CA), and single-turnover GTP hydrolysis was followed at 37°C. Control experiments showed that the Op18 preparations used neither bind nor hydrolyze [α-^{32}P]GTP. Nucleotide hydrolysis was quantitated by ascending chromatography as described (Austin and Dixon, 1992).

MT Assembly

The assembly of individual MTs seeded from axoneme fragments was visualized using video-enhanced differential interference contrast (DIC) microscopy as described (Howell *et al.*, 1999b). Assembly conditions were such that MTs assembled only from axonemes and the total amount of tubulin incorporated into MT polymer were insignificant compared with the total tubulin concentration. The buffers used in the present study were PEM buffers adjusted to either pH 6.8 or pH 7.5.

RESULTS

Interphase and Mitotic Phenotypes of Pseudophosphorylated Op18

Op18 is phosphorylated to high stoichiometry at mitosis, which results in its inactivation (Marklund *et al.*, 1996; Larsson *et al.*, 1997). Hence, due to mitotic phosphorylation, ectopic expression of wild-type Op18 (Op18-wt) destabilizes the interphase array of MTs without interfering with spindle formation during mitosis. However, the Op18-tetraA, a mutant with all four Ser-phosphorylation sites substituted with Ala is nonphosphorylatable and therefore constitutively active, and ectopic expression blocks formation of the mitotic spindle (Marklund *et al.*, 1996). A general assumption is that the effect of Ser-to-Ala substitutions reflects only lack of phosphorylation of a particular site in intact cells, and that the Ala substitutions per se have no other effects. Substitutions of a Ser-phosphorylation site with a negatively charged Glu residue, on the other hand, is expected to provide at least a partial mimic of a negatively charged phosphate group. A mutant of Op18 with all four Ser-phosphorylation sites substituted with Glu (termed Op18-tetraE in this study) has been variously reported to be either active or inactive, depending on the in vivo or in vitro assay system used (Curmi *et al.*, 1997; Horwitz *et al.*, 1997; Gavet *et al.*, 1998; Larsson *et al.*, 1999a).

Using a conditional shuttle-vector based expression system, Op18-wt, Op18-tetraA, and Op18-tetraE were overexpressed in the human K562 leukemia cell line, and Op18

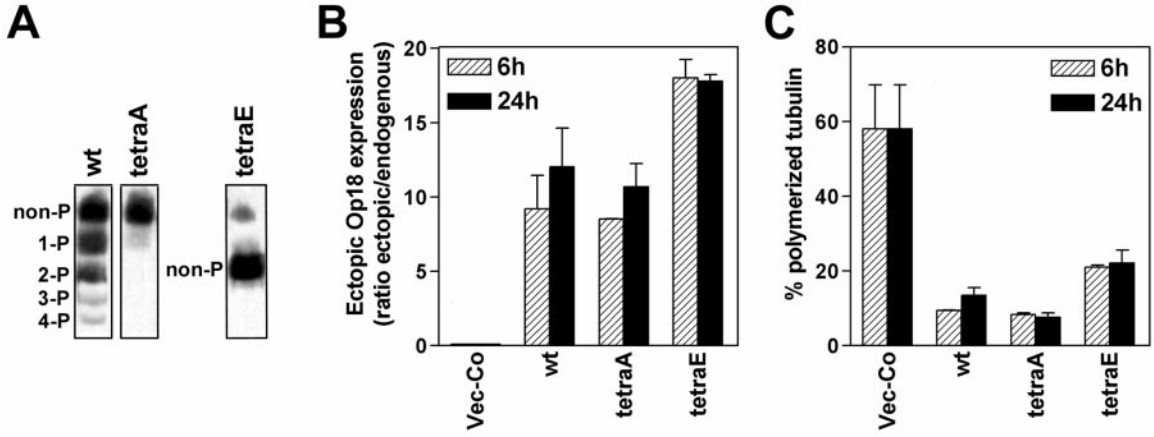

Figure 1. Expression and MT regulatory properties of nonphosphorylatable Ala- and Glu-substituted Op18 mutants. K562 cells were transfected with 12 μg DNA of each of the indicated pMEP4 derivatives, and hygromycin resistant cell lines were selected and induced with Cd^{2+} (0.05 μM), as described in MATERIALS AND METHODS. (A) Transfected cell lines were Cd^{2+} induced for 24 h and phosphoisomers of Op18 were resolved by native PAGE and revealed using antibodies toward the C-terminus of Op18 (up to four Ser sites, Ser-16, Ser-25, Ser-38 and Ser-63, are phosphorylated in vivo). The faint band, at the position of Op18-tetraA that is observed in the lane depicting migration of Op18-tetraE, represents endogenous Op18. (B) Op18 levels were determined after 6 and 24 h of Cd^{2+} induction and data are presented as fold induction over endogenous Op18 (the endogenous Op18 level in K562 cells is $\sim$ 10 μM). (C) The fraction of polymerized tubulin in cells treated as under (B). Panels B and C show the mean of two independent transfection experiments.

phosphoisomers were analyzed by native PAGE (Figure 1A). It is evident that Op18-wt is expressed as a mixture of non-, mono-, di- and traces of tri- and tetra-phosphorylated proteins. As expected, Op18-tetraA and Op18-tetraE are nonphosphorylated and migrate as single bands (note that 4 negatively charged Glu residues of Op18-tetraE alter the migration and that the faint, slow migrating band at the top is endogenous Op18). Quantification of expression levels after 6 and 24 h of Cd^{2+} induced expression showed rapid and high expression of all three derivatives (Figure 1B). Analysis of MT polymerization status in transfected cells revealed that all three Op18 derivatives caused a major collapse of the MT-system. However, the severity of the disorder caused by Op18-tetraA and Op18-wt is clearly stronger than the disorder caused by Op18-tetraE. Induced expression of all Op18 derivatives results in depolymerization of MTs within 6 h of induced expression. Given the division time of K562 of $\sim$ 20 h, the data at 6 h reflect mainly MT-destabilization during the interphase of the cell cycle.

To determine if ectopic Op18-tetraE allows formation of the mitotic spindle, the DNA profiles of Op18 transfected cells were analyzed (Figure 2). As expected from phosphorylation-inactivation of Op18 during mitosis (Marklund *et al.*, 1996), Op18-wt does not alter the cell cycle distribution, while Op18-tetraA causes an almost complete mitotic block at 24 h, followed by mitotic slippage and endoreduplication after 72 h of induced expression. The observed effect after 72 h is due to a defect in the metaphase checkpoint of K562,

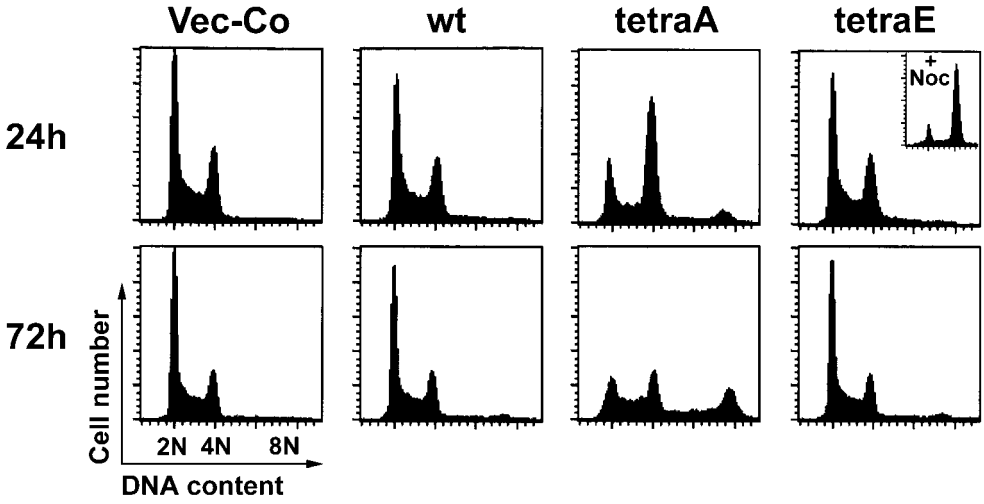

Figure 2. Cell cycle phenotypes of wild-type and kinase target site deficient mutants of Op18. K562 cells were transfected, and hygromycin resistant cell lines were selected as in Figure 1. (A) Op18 expression was thereafter induced with Cd^{2+} (0.05 μM) for 24 h (upper panels) or 72 h (lower panels). DNA was stained with propidium iodide and analyzed by flow cytometry. The insert in the upper right panel shows the effect of nocodazole (0.5 μM) on Op18-tetraE expressing cells. Data are representative for three independent experiments.

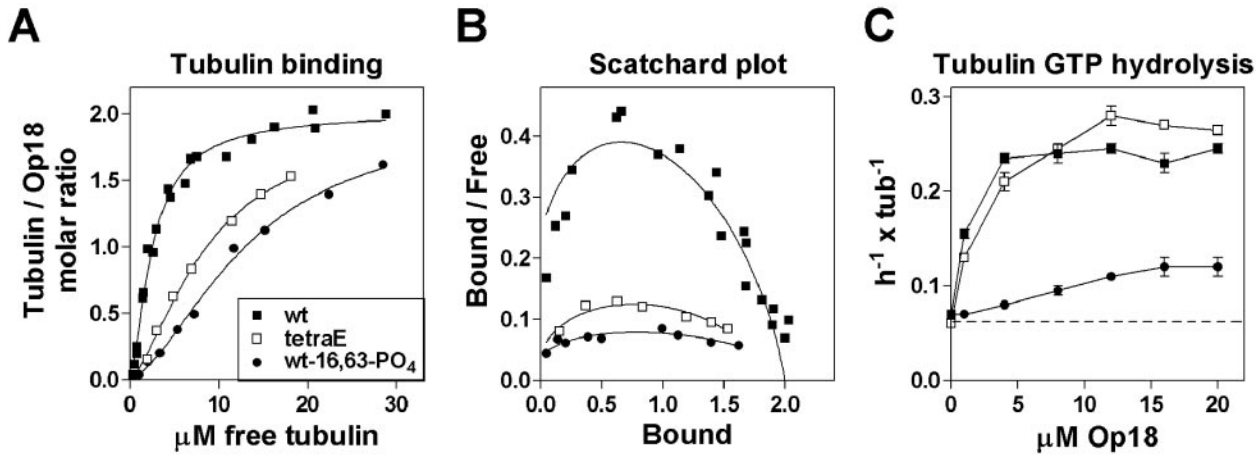

Figure 3. Glu-substitutions only partially mimic phosphorylation-inactivation of tubulin-directed in vitro activities of Op18. (A) Op18-tubulin equilibrium binding curves were determined at pH 7.5 for Op18-wt, Op18-tetraE and Ser-16 and Ser-63 phosphorylated Op18 (Op18–16,63-PO_4) as described in MATERIALS AND METHODS. The contribution of nonspecific binding (3% of free tubulin) is subtracted. Curves assuming two-site positive cooperative binding were fitted to the data points. (B) Scatchard conversions of the binding curves. (C) Hydrolysis of [α^{32}P]GTP preloaded onto tubulin (3 μM) was determined at various concentrations of the indicated Op18 derivatives. Data are representative for at least two independent experiments.

which is frequently observed among malignant cells (Cahill *et al.*, 1999). Importantly, Op18-tetraE expression causes essentially no alteration of the cell cycle profile. This is not due to a general cell cycle arrest, since Op18-tetraE expressing cells readily accumulate in mitosis in the presence of the MT-directed drug nocodazole (see insert in Figure 2).

Functional Dissection of Op18-tetraE and Phosphorylated Op18

The data above suggest that the pseudophosphorylated Op18-tetraE derivative lacks a property essential for interference with spindle formation, while still retaining properties that destabilize the MT-system during the interphase. This contrasts to authentic phosphorylation, which blocks all detectable MT-destabilizing activity of Op18 during both interphase and mitosis (Marklund *et al.*, 1996; Larsson *et al.*, 1997; Gradin *et al.*, 1998). It was therefore of interest to compare the profiles of MT/tubulin-directed in vitro activities of Op18-tetraE with Op18-wt phosphorylated on Ser-16 and Ser-63. Dual phosphorylation on these two sites had previously been shown to be sufficient to attenuate the MT-destabilizing activity of Op18 in intact cells (Gradin *et al.*, 1998).

Equilibrium binding analysis of Op18-wt, Op18-tetraE, and phosphorylated Op18 shows that all bind two tubulin heterodimers by a mechanism involving two-site positive cooperativity (Figure 3A and B, and Table 1). This implies that all derivatives bind the first tubulin with low affinity, which generates a second high affinity-binding site and a subsequent formation of a ternary tubulin$_2$-Op18 complex. Glu-substitution results in a 3- to 4-fold decrease in the tubulin-affinity, which is in agreement with the 3-fold decrease estimated by plasmon resonance measurement (Curmi *et al.*, 1997), and most importantly, the difference between Op18-tetraE and phosphorylated Op18 is only ~ 2-fold (see summary of calculated affinities, Table 1). To characterize modulation of the stability of Op18-tubulin interactions by phosphorylation and Glu-substitutions, we determined the dissociation rates. The data in Table 2 shows that Op18-tubulin complexes rapidly dissociate upon dilution, and as expected from the reported pH regulation of binding affinity (Curmi *et al.*, 1997), dissociation is more rapid at the higher pH (compare data obtained at pH 6.8 and pH 7.5). As anticipated from decreased binding affinities, both phosphorylation and Glu-substitutions result in increased dissociation rates. It is notable that the difference in dissociation rates between Op18-tetraE and phosphorylated Op18 is modest and that the relative differences in dissociation rates are very similar at both pH 6.8 and pH 7.5 (see relative $T_{1/2}$ values, Table 2).

In contrast to tubulin binding characteristics described above, there is a major difference in the potency with which Op18-tetraE and phosphorylated Op18 stimulate tubulin GTPase activity (Figure 3C). Thus, the Glu-substitutions have no detectable effect, while authentic phosphorylation

Table 1. Modulation of Op18-tubulin binding affinities by phosphorylation and Glu-substitution of phosphorylation sites

	$K_d1 \pm$ SE (μM)	$K_d2 \pm$ SE (μM)	Free [tubulin] at Half saturation of Op18 (μM)
Op18-wt	7.2 ± 1.9	0.9 ± 0.3	2.5
Op18-tetraE	27 ± 7.2	2.7 ± 1.3	8.8
Op18-wt-16,63-PO_4	61 ± 23	2.9 ± 1.8	13.4

Equilibrium dissociation constants at pH 7.5 were calculated according to a two-site positive co-operativity model and are based on the data shown in Figure 3, A and B. The free tubulin concentration at half saturation was estimated from curves fitted according to a two-site cooperativity model.

Table 2. Modulation of Op18-tubulin dissociation rates by phosphorylation and Glu-substitution of phosphorylation sites

	pH	k ± SE (s^{-1})	$T_{1/2}$ ± SE (s)	Relative $T_{1/2}$ values (% of Op18-wt)
Op18-wt	6.8	0.0068 ± 0.0007	102 ± 10.2	100 (pH 6.8)
Op18-tetraE	6.8	0.0158 ± 0.0012	44 ± 3.3	43
Op18-wt-16,63-PO_4	6.8	0.0249 ± 0.0010	28 ± 1.2	27
Op18-wt	7.5	0.0099 ± 0.0007	70 ± 5.1	100 (pH 7.5)
Op18-tetraE	7.5	0.0248 ± 0.0027	28 ± 3.0	40
Op18-wt-16,63-PO_4	7.5	0.0387 ± 0.0023	18 ± 1.1	26

Determination of dissociation rates, expressed as either k (s^{-1}) or half-lives ($T_{1/2}$, s) of Op18-tubulin complexes was determined at pH 6.8 and pH 7.5, assuming one-phase exponential decay as described in MATERIALS AND METHODS.

results in almost complete attenuation of tubulin GTPase stimulatory activity, even at high Op18 concentration. This indicates an important difference between Glu substitution and authentic phosphorylation that cannot be attributed to differences in tubulin binding affinities.

A recent study (Howell *et al.*, 1999b), which involved in vitro MT assembly assays, showed that Op18 has a specific plus end directed catastrophe-promoting activity at pH 7.5, while an MT growth rate inhibitory activity that does not discriminate between plus and minus ends (i.e., sequestering-like activity) predominates at pH 6.8. It is evident from Figure 4A that Op18-tetraE shows activity similar to Op18-wt with respect to inhibition of growth rate at pH 6.8. In agreement with earlier results (Howell *et al.*, 1999b), Op18 does not inhibit growth rate at pH 7.5. Interestingly, however, Glu-substitutions abolish the specific plus end directed catastrophe-promoting activity of Op18 (Figure 4B). The corresponding analysis of phosphorylated Op18 reveals attenuation of both growth rate inhibition at pH 6.8 and catastrophe activity at pH 7.5 (Figure 5).

In conclusion, both Glu-substitutions and authentic phosphorylation on Ser-16 and Ser-63 attenuate the catastrophe-promoting activity of Op18. However, the Op18-tetraE derivative retains MT growth rate inhibitory activity and efficiently stimulates the intrinsic tubulin GTPase activity. The effect of either phosphorylation or Glu-substitution on tubulin binding is significant; however, it is insufficient to explain differences in the in vitro activity profiles. Hence, it appears that Glu-substitutions result in selective attenuation of the catastrophe-promoting activity of Op18.

Nonphosphorylatable Truncation Mutants Link the Catastrophe-promoting Activity of Op18 to Disruption of the Mitotic Spindle

The apparently selective loss of in vitro catastrophe activity of Op18-tetraE suggested that disruption of the mitotic spindle by nonphosphorylatable Op18 derivatives may require the catastrophe-promoting activity of Op18, while other MT-destabilizing activities of Op18 are sufficient for a substantial destabilization of interphase microtubules. With respect to regulation of the dynamic properties of MTs measured in vitro, Op18-tetraE closely resembles an N-terminal truncation derivative of Op18. Thus, in a previous in vitro study of MT assembly, analysis of Op18-Δ4–24-F revealed that the catastrophe-promoting activity, but not the MT growth rate inhibitory activity, requires the N-terminal region of Op18 (Howell *et al.*, 1999b). To determine if the catastrophe-promoting activity of overexpressed nonphosphorylatable Op18 was required for disruption of the mitotic spindle, truncation derivatives of Op18 were substituted at Ser-phosphorylation sites with Ala residues and expressed in K562 cells. One derivative, termed Op18-Δ4–24-tetraA-F, is catastrophe-deficient while the other, termed Op18-Δ100–147-tetraA-F, is catastrophe-proficient but lacks MT growth rate inhibitory activity in vitro (Howell *et al.*, 1999b). Analysis on a native gel confirmed that the expressed proteins were nonphosphorylatable because the two truncated derivatives, as well as the full-length Flag epitope-tagged version of Op18 (Op18-tetraA-F), migrated as single bands (Figure 6A). The transfection and expression conditions used resulted in comparable expression levels of the two truncated proteins and Op18-tetraA-F (Figure 6B).

The phenotypes of transfected cells were analyzed on the level of MT polymerization status and cell cycle profiles. Analysis of MT-polymerization status, which at the 6-h time-point primarily reflects activities in interphase cells, reveals somewhat decreased activities of both N- and C-terminally truncated Op18, but both derivatives still cause a rapid and dramatic MT-destabilization (Figure 6C). Most importantly, analysis of cell cycle profiles demonstrated a clear-cut difference between the two nonphosphorylatable truncated derivatives, as only the catastrophe-promoting Op18-Δ100–147-tetraA-F derivative caused a mitotic block, followed by mitotic slippage and endoreduplication (Figure 7). The apparent lack of mitotic block in Op18-Δ4–24-tetraA-F expressing cells was not due to a general cell cycle arrest or potential interference with a metaphase checkpoint, because transfected cells readily accumulated in mitosis in the presence of the MT-directed drug nocodazole (see insert in Figure 7). Moreover, dual analysis of Op18 expression and DNA content by flow cytometry showed that Op18-Δ4–24-tetraA-F, as well as Op18-TetraE and the other derivatives employed in this study, was evenly expressed throughout the cell cycle (data not shown). This excludes mitosis specific degradation as the mechanism behind selective disruption of interphase MTs.

To determine the severity of the phenotype of nonphosphorylatable Op18-derivatives, spindle morphologies were manually inspected and graded into three classes (normal and abnormal type I and II) described and depicted in Figure 8. The percentage of normal versus abnormal spindles was quanti-

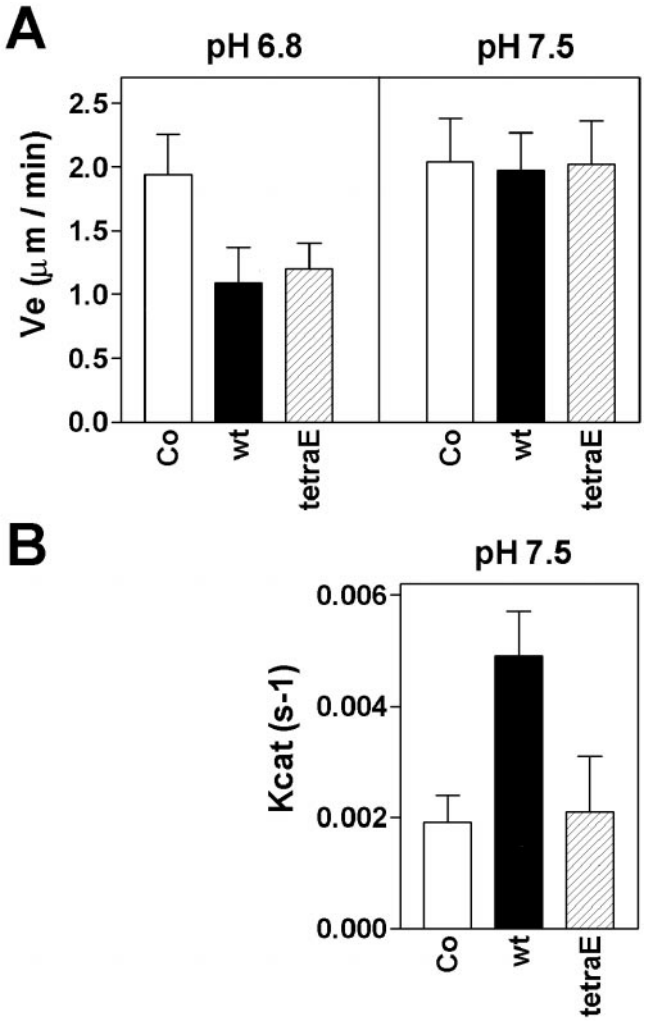

Figure 4. Analysis of MT plus end dynamics reveals that the Op18-tetraE mutant retains the MT growth rate inhibitory activity at pH 6.8 but has lost specific catastrophe-promoting activity at pH 7.5. (A) Elongation velocity at the plus end for MTs assembled at pH 6.8 or pH 7.5 with 11 μM tubulin alone (open bars) or 11 μM tubulin plus 1.7 μM of Op18-wt (black bars) or Op18-tetraE (shaded bars). (B) Catastrophe frequencies at MT plus ends measured at pH 7.5 in the same experiment, as shown in panel A. Data for tubulin alone and in the presence of Op18-wt have previously been published (Howell *et al.*, 1999b), but are shown here for comparison. Values represent means +/-SD.

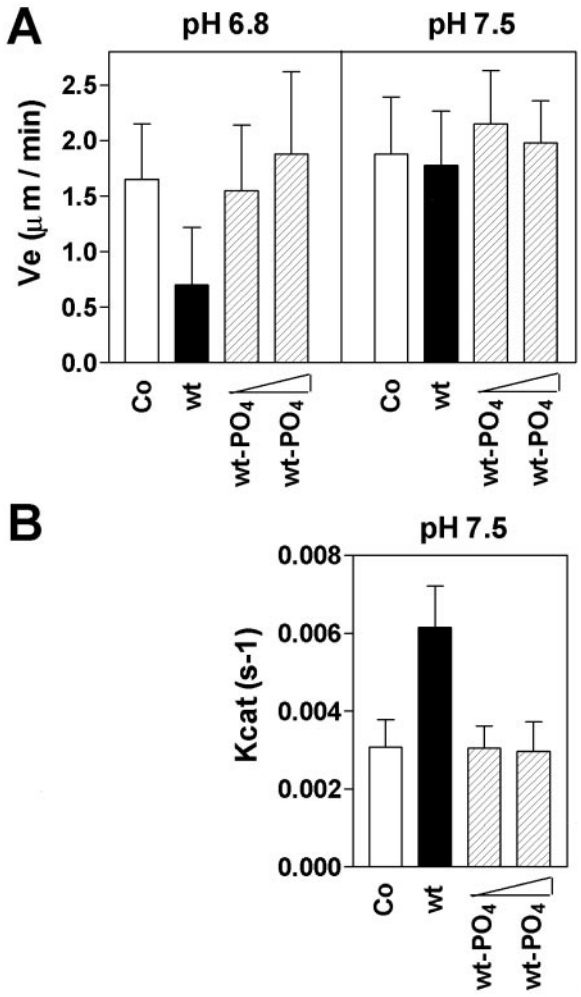

Figure 5. Op18 phosphorylations attenuate both the MT growth rate inhibitory activity at pH 6.8 and the specific catastrophe-promoting activity at pH 7.5. (A) Elongation velocity at plus ends for MTs assembled at pH 6.8 and pH 7.5 with 11 μM tubulin alone (open bars), or 11 μM tubulin plus 2 μM nonphosphorylated Op18-wt (black bars), or 2 μM and 5 μM Ser-16 and Ser-63 phosphorylated Op18 (Op18–16, 63-PO_4, shaded bars). Op18-wt mean growth rate at pH 6.8 is significantly different from all other rates ($p < 0.05$), while tubulin alone, 2 and 5 μM Op18–16, 63-PO_4 mean growth rates are not significantly different. (B) Catastrophe frequency at MT plus ends measured at pH 7.5 in the same experiment as shown in panel A. Data represent means $\pm$SD. Data shown in Figures 4 and 5 are obtained using different tubulin preparations, which explain the slight difference in dynamic properties.

tated and normalized to the frequency of mitotic cells, as defined by flow cytometry (Table 3). The data show that ectopic expression of Op18-wt, Op18-Δ4–24-tetraA-F, and Op18-tetraE resulted in a small increase in the fraction of mitotic cells, but the frequency of cells with abnormal spindles was still low. In contrast, ectopic expression of Op18-Δ100–147-tetraA-F results in a major increase in metaphase cells. A large fraction of these cells contained type I abnormal spindles, which is likely the cause of the mitotic block. Expression of full-length Op18-tetraA resulted in the most extreme appearance of mitotic cells, which to a large extent lacked detectable MT structures (i.e., abnormal type II).

Taken together, the DNA profile reveals that Op18-Δ100–147-tetraA-F retains potent metaphase checkpoint activating properties, but it is still clear from morphological analysis that the C-terminal truncation results in loss of a property that contributes to the severity of mitotic spindle disruption. Nevertheless, it appears that the mitotic spindle is primarily sensitive to the catastrophe-promoting activity of Op18, because nonphosphorylatable catastrophe-deficient Op18-derivatives interfere minimally with formation of mitotic spindles. It follows that formation of the mitotic spindle is

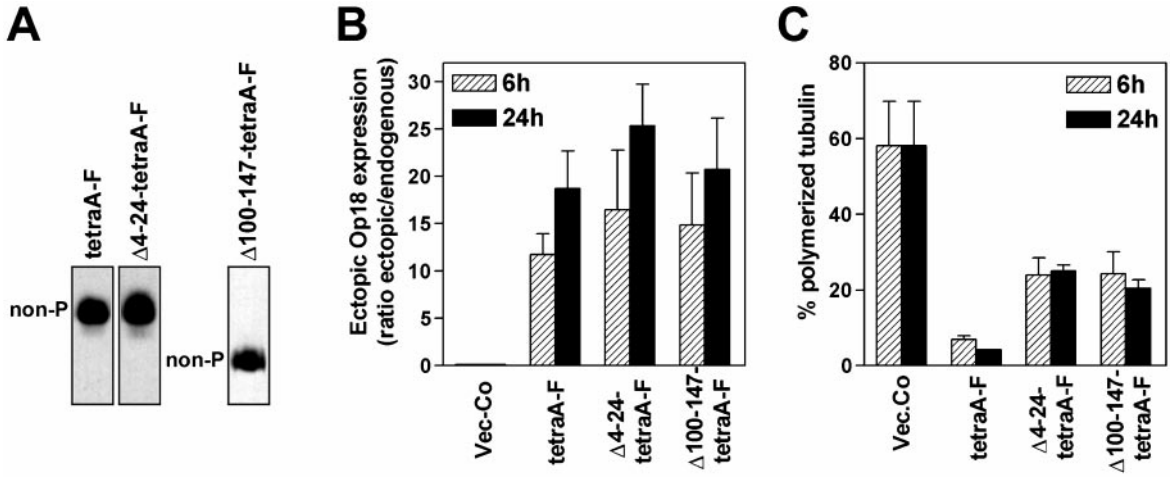

Figure 6. Nonphosphorylatable Ala-substituted Op18 deletion derivatives can be used as probes to distinguish interphase and mitotic MTs. K562 cells were transfected, and hygromycin resistant cell lines were selected as in Figure 1 and induced with Cd^{2+} (0.5 μM) for the indicated time. To obtain comparable expression levels of the indicated Flag-epitope tagged Op18 derivatives, DNA concentrations were adjusted as indicated in MATERIALS AND METHODS. (A) Transfected cell lines were Cd^{2+} induced for 24 h, and phosphoisomers of Flag-epitope tagged Op18 were resolved by native PAGE and revealed using antibodies toward the epitope tag. The expressed derivatives migrate at similar positions, as the corresponding *E. coli* produced derivatives (data not shown). (B) Op18 levels were determined after 6 and 24 h of Cd^{2+} induction, and data are presented as fold induction over endogenous Op18 ($\sim$ 0 μM). (C) The fraction of polymerized tubulin in the cells shown in (B). Panels B and C show the mean of two independent transfection experiments.

relatively resistant to other, as yet uncharacterized, activities of Op18 that destabilizes interphase MTs.

DISCUSSION

Alteration at the N-Terminal Region Can Result in Selective Loss of Catastrophe-promoting Activity

Here, we describe the phenotypes of distinct types of Op18 mutants in vitro and in intact cells during interphase and mitosis. Two of the mutants analyzed, Op18-tetraE and Op18-Δ4–24, have alterations that affect the N-terminal region of the protein. Both of these mutants share a specific defect, namely an apparently selective loss of catastrophe-promoting activity. The combined evidence from this and previous studies shows that Glu-substitution and N-terminal deletion of Op18 have similar phenotypic outcome. First, like Op18-wt, both types of mutants bind two tubulins according to a two-site positive cooperativity model, but with some decrease in binding affinity (Larsson *et al.*, 1999b and Table 1). Second, neither mutation has an effect on stimula-

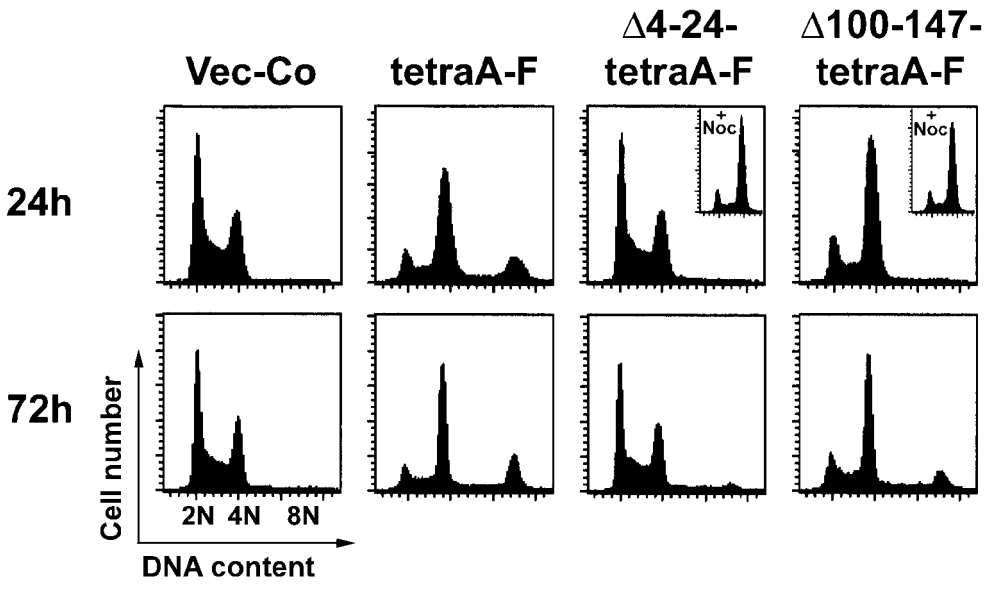

Figure 7. Cell cycle phenotypes of nonphosphorylatable Ala-substituted Op18 deletion derivatives suggest that catastrophe-promotion is essential for a mitotic block. K562 cells were transfected and hygromycin resistant cell lines were selected as in Figure 1. (A) Op18 expression was induced with Cd^{2+} for 24 h (upper panels) or 72 h (lower panels). DNA was stained with propidium iodide and analyzed by flow cytometry. The inserts in two of the upper panels show G2/M block after 24 h in presence of nocodazole (0.5 μM). Data are representative for two independent experiments.

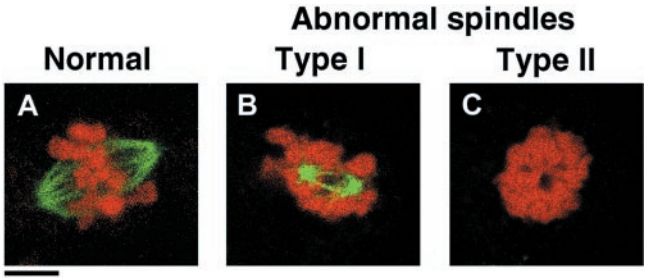

Figure 8. The mitotic phenotypes of nonphosphorylatable Ala-substituted Op18 truncation derivatives. K562 cells were transfected, and hygromycin resistant cell lines were selected and induced with Cd^{2+} as in Figure 1. After 24 h, cells were fixed and double stained with anti-α-tubulin (green color) and propidium iodide DNA staining (red color). Representative examples of normal and abnormal metaphase cells, observed using laser scanning confocal microscopy, are shown. (A) Shows a typical normal metaphase cell, (B) shows a type I mitotic figure that lacks most kinetochore MTs; MTs appear as small star-like asters. Most cells contain two asters, suggesting that the centrosomes are separated. In addition, all the condensed chromosomes appear aggregated. (C) Type II mitotic figures represent the most severe defect, since MT structures were undetectable and the condensed chromosomes are aggregated. Bar, 4 μm.

tion of soluble tubulin GTP hydrolysis (Larsson *et al.*, 1999b and Figure 3). Third, both mutants retain the ability to inhibit the tubulin polymerization rate, but they have lost specific catastrophe-promoting activity in vitro (Howell *et al.*, 1999b and Figure 4), and both are potent inhibitors of taxol-driven in vitro polymerization of MTs (Larsson *et al.*, 1999a and data not shown). Most interestingly, the present study in intact cells reveals that the interphase MT-destabilizing activity of both mutants is to a large extent retained, but these mutants do not interfere significantly with spindle formation.

The observed MT-destabilization by Op18-tetraE may appear to be in conflict with two previous reports. In one report it was shown that Asp substitutions at phosphorylation sites inhibited the MT-destabilizing activity of Op18, as analyzed by microinjection of nocodazole pretreated COS-7 cells (Horwitz *et al.*, 1997). In the other report it was shown that Glu substitutions at phosphorylation sites inhibited the MT-destabilizing activity of Op18 when transiently expressed in HeLa cells (Gavet *et al.*, 1998). However, in these two studies, which relied on manual inspection of cells, significant Op18 mediated decreases of the MT-network could only be detected in a fraction of successfully microinjected/transfected cells (58.8% of Op18-wt injected COS-7 cells and ~37% of Op18-wt expressing HeLa cells). The genetic system employed here is clearly more sensitive as flow cytometric analysis reveals a dramatic (80–90% on average) destabilization of MTs in almost all cells within 6 h of induced expression of Op18-wt (Larsson *et al.*, 1999a). Using this system, it is evident that Op18-tetraE has a significantly decreased MT-destabilizing activity as compared with Op18-wt, but flow cytometric analysis still reveals a clear-cut activity of this derivative in interphase cells (Figure 1), which was confirmed by images of individual cells (Larsson *et al.*, 1999a). Hence, high and homogeneous expression levels, together with flow cytometric analysis of MT content, allow detailed comparison of partially inactivated Op18-derivatives.

Pseudophosphorylation by Glu-Substitutions Only Partially Mimics Activity-Attenuation by Authentic Phosphorylation

Nonphosphorylatable derivatives of Op18 are generated by substitutions of phosphorylation sites with Ala residues with the assumption that the effects of Ser to Ala substitutions only reflect lack of phosphorylation of particular sites in intact cells. A mutant with phosphorylation sites substituted with negatively charged Glu residues are prepared with the assumption that these substitutions provide at least a partial mimic of phosphorylation. The phenotype of the Op18-tetraE mutant, as outlined above, is clearly different from the effect of authentic phosphorylation. Combined results from previous reports are in line with this conclusion. For example, phosphorylations, but not Glu-substitutions, attenuate the inhibitory activity of Op18 during taxol-driven MT polymerization (Larsson *et al.*, 1997, 1999a). In the present study, the effect of Glu-substitutions of the four phosphorylation sites was compared with the effect of phosphorylation on Ser-16 and Ser-63 of Op18. In both

Table 3. Summary of the mitotic phenotypes of nonphosphorylatable Ala-substituted Op18 deletion derivatives

			Abnormal Spindles[b]	
	Total Mitotic Index[a] (%)	Normal Spindles (%)	Type I (%)	Type II (%)
Vec-Co	4.7	4.6	<0.5	<0.5
Op18-wt	8.8	8.2	0.6	<0.5
Op18-tetraA	51.4	1.0	9.4	41.0
Op18-tetraE	11.1	7.9	3.2	<0.5
Op18-Δ4-24-tetraA-F	9.3	7.5	1.9	<0.5
Op18-Δ100-147-tetraA-F	38.4	10.3	25.4	2.7

[a] DNA and MPM-2 dual parameter staining in combination with flow-cytometry was used to determine the frequency of mitotic cells.

[b] Normal and abnormal (type I and II) mitotic figures were evaluated as described in Figure 8. The percentage of each type of mitotic figure was normalized to the frequency of mitotic cells. The data are derived from observations of at least 200 mitotic cells.

cases, four negative charges are introduced into the N-terminal part of Op18. Phosphorylation causes a somewhat more pronounced decrease in Op18-tubulin binding affinity than Glu-substitution (~ 2-fold, Table 1), but similar to nonphosphorylated Op18 and Op18-tetraE, phosphorylated Op18 bound two tubulins according to a two-site positive cooperativity model. Because Op18-tetraE retains full tubulin GTPase stimulatory activity, the twofold difference in binding affinity cannot explain the virtual lack of GTPase stimulatory activity of phosphorylated Op18. Moreover, it also seems unlikely that decreased binding can explain that phosphorylation attenuates growth rate inhibition during MT assembly at pH 6.8, since Op18-tetraE was in this respect indistinguishable from nonphosphorylated Op18 (compare Figures 4 and 5).

The binding data presented in this study contrast with results from chemical cross-linking assessment of the effect of Op18 phosphorylation on tubulin binding-affinity (Larsson *et al.*, 1997; Gradin *et al.*, 1998). Using chemical cross-linking it appeared that dual phosphorylation on Ser-16 and Ser-63 had a major inhibitory impact on tubulin binding, which was interpreted in favor of a mechanistic model where phosphorylation-inactivation can be explained by loss of tubulin complex formation (Lawler, 1998; Andersen, 1999). However, as argued above, the current quantitative binding analyses and comparisons of activity-profiles of Op18-tetraE and phosphorylated Op18 argues strongly against such a simple model for phosphorylation-inactivation of Op18.

Phosphorylation-inactivation of Op18 in intact cells has previously been evaluated by a genetic system allowing conditional coexpression of constitutively active cognate kinases and a series of kinase target-site deficient mutants of Op18. The results show that phosphorylation of Op18 on Ser-16 and Ser-63 is sufficient to switch off virtually all Op18 activity in intact cells (Gradin *et al.*, 1998). The approximate intracellular concentration of ectopic Op18 in these experiments was around 50–100 μM, which exceeds the estimated intracellular tubulin concentration (~ 20 μM) in K562 cells (Larsson *et al.*, 1999b). Given the binding data reported in the present study (Figure 3A and Table 1 and 2) and the high intracellular Op18 and tubulin concentrations, which by far exceed concentrations used for in vitro experiments, it is difficult to envision that the modest phosphorylation-regulation of tubulin binding affinity is sufficient to result in attenuation of Op18 activity in transfected cells. This line of argumentation is supported by the phenotype of Op18-tetraE, which differs only twofold in tubulin binding affinity from phosphorylated Op18 but still efficiently destabilizes interphase MTs (Figure 1). Hence, in agreement with in vitro experiments, we conclude that phosphorylations, but not Glu-substitutions, have the potential to attenuate both catastrophe-promotion and the poorly defined MT-destabilizing activity associated with the C-terminal part of Op18, and furthermore, that this attenuation cannot be accounted for by phosphorylation-regulation of Op18-tubulin binding affinity in intact cells.

Differential Sensitivity of Interphase and Mitotic MTs to Distinct Activities of Op18

A recent study has shown that the catastrophe-promoting Op18-Δ100–147-F derivative is severely affected in its tubulin-binding affinity but still exerts a potent MT-destabilizing activity in intact cells, which is independent of binding to tubulin dimers (Larsson *et al.*, 1999b). Evidence for catastrophe-promoting activity in intact cells was obtained by analysis of MT density in the lamella region of microinjected newt lung cells, as the observed lamella clearing indicated the expected shortening of MTs indicative of a catastrophe factor (Larsson *et al.*, 1999b). This suggests that at least the catastrophe-promoting activity of Op18 is independent of interaction with free tubulin, and it follows that the mechanism may involve interactions with MT ends. Here the cell cycle phenotype of a nonphosphorylatable derivative, Op18-Δ100–147-tetraA-F, was compared with two distinct catastrophe-deficient and nonphosphorylatable derivatives of Op18, namely Op18-tetraE and Op18-Δ4–24-tetraA-F. The data show that these mutants have differential activities toward mitotic and interphase MTs, which is in line with previous genetic evidence that Op18 mediates at least two MT-directed activities in intact cells (Larsson *et al.*, 1999b). Analysis of DNA-profiles suggested that the mitotic spindle was completely resistant to destabilization by catastrophe-deficient mutants, and examination of mitotic figures revealed only a minor interference with the mitotic spindle (Table 3). In contrast, catastrophe-proficient Op18-Δ100–147-tetraA-F blocked essentially all cells in mitosis, and most cells showed visual defects in their mitotic spindles. However, the defects were not as dramatic as that caused by expression of the full-length Op18-tetraA-F derivative, which resulted in the virtual absence of detectable spindle MTs. Thus, the as yet undefined activities that require an intact C-terminus are insufficient in themselves to block spindle formation, but these activities can clearly cooperate with the catastrophe-promoting activity of Op18 to obstruct the MT-system during mitosis.

How Does Op18 Decrease Interphase MT Content in the Absence of Catastrophe-Activity?

At present we can only speculate concerning the nature of the activity that is absent in C-terminally truncated but present in N-terminally truncated and Glu-substituted derivatives. Based on in vitro assembly assays, this activity correlates with inhibition of growth rate at pH 6.8, which was at that time interpreted to suggest a tubulin sequestering-like activity (Howell *et al.*, 1999b and Figure 4). If tubulin sequestering is involved in the mechanism by which Op18-tetraE and Op18-Δ4–24-tetraA-F selectively destabilize interphase MTs, it follows that mitotic MTs would be insensitive to such a tubulin sequestering mechanism. This seems unlikely and, as argued above and in a previous report (Larsson *et al.*, 1999b), a potential sequestering activity of Op18 appears to play a minor role in intact cells. For example, the concentration of endogenous Op18 (~ 10 μM) in K562 leukemia cells is sufficient to form ternary complexes with essentially all cellular tubulin (~ 20 μM) (Larsson *et al.*, 1999b). By analyzing Op18-tubulin interactions in crude extracts of transfected K562 cells, we have previously shown that ectopic N-terminally truncated Op18 shows very low levels of association with endogenous tubulin. This could be explained by decreased tubulin binding-affinity of truncated Op18, as this results in endogenous Op18 out-competing binding in a crude extract (Larsson *et al.*, 1999b). Hence, it seems unlikely that tubulin sequestering is responsible for the as yet undefined MT-destabilizing activity of Op18-Δ4–24-F.

In summary, the present study shows that catastrophe-promotion by Op18 is sufficient to disrupt the mitotic spindle, while the activity that requires an intact C-terminus of Op18 destabilizes primarily the interphase network of MTs. This suggests functional differences between interphase and mitotic MTs, which may be the result of differential binding of MAPs during these two cell cycle stages (reviewed by Cassimeris, 1999). Our results confirm that Op18 exerts at least two distinct activities in intact cells, and an important goal will be to elucidate the nature of the activity associated with the C-terminal region of Op18. If this can be achieved, the nonphosphorylatable/constitutively active Op18 mutants characterized in this report will become even more interesting tools to dissect functional differences between the MT-system during interphase and mitosis.

ACKNOWLEDGMENTS

We thank V. Shingler for helpful discussions and K. Fridell for assistance with in vitro phosphorylations. P.H., N.L., B.S., and M.G. were supported by Swedish Natural Science Research Council and the Swedish Society for Medical Research. B.H., L.C., and J.M. were supported by a grant from the National Institutes of Health.

REFERENCES

Andersen, S.S. (1999). Balanced regulation of microtubule dynamics during the cell cycle: a contemporary view [published erratum appears in Bioessays 1999; *21,* 363]. Bioessays *21*, 53–60.

Austin, S., and Dixon, R. (1992). The prokaryotic enhancer binding protein NTRC has an ATPase activity which is phosphorylation and DNA dependent. EMBO J. *11*, 2219–2228.

Belmont, L.D., and Mitchison,T.J. (1996). Identification of a protein that interacts with tubulin dimers and increases the catastrophe rate of microtubules. Cell *84*, 623–631.

Brattsand, G., Roos, G., Marklund, U., Ueda, H., Landberg, G., Nanberg, E., Sideras, P., and Gullberg, M. (1993). Quantitative analysis of the expression and regulation of an activation-regulated phosphoprotein (oncoprotein 18) in normal and neoplastic cells. Leukemia*7*, 569–579.

Cahill, D.P., Kinzler, K.W., Vogelstein, B., and Lengauer, C. (1999). Genetic instability and darwinian selection in tumors. Trends. Cell. Biol. *9*, M57–M60.

Cassimeris, L. (1999). Accessory protein regulation of microtubule dynamics throughout the cell cycle. Curr. Opin. Cell. Biol. *11*, 134–141.

Curmi, P.A., Andersen, S.S., Lachkar, S., Gavet, O., Karsenti, E., Knossow, M., and Sobel, A. (1997). The stathmin/tubulin interaction in vitro. J. Biol. Chem. *272*, 25029–25036.

Deacon, H.W., Mitchison, T.J., and Gullberg, M. (1999) Op18/stathmin, Part 2. Tubulin and associated proteins. In: Guidebook to the Cytoskeletal and Motor Proteins.2nd ed. Eds., Kreis, T. and Vale, Oxford, UK: Oxford University Press, 222–225.

Desai, A., and Mitchison, T.J. (1997) Microtubule polymerization dynamics. Ann. Rev. Cell Dev. Biol. *13*, 83–117.

Gavet, O., Ozon, S., Manceau, V., Lawle, S., Curmi, P., and Sobel, A. (1998). The stathmin phosphoprotein family: intracellular localization and effects on the microtubule network. J. Cell. Sci. *Pt 22*, 3333–3334.

Gradin, H.M., Larsson, N., Marklund, U., and Gullberg, M. (1998). Regulation of microtubule dynamics by extracellular signals: cAMP-dependent protein kinase switches off the activity of oncoprotein 18 in intact cells. J. Cell. Biol. *140*, 131–141.

Gradin, H.M., Marklund, U., Larsson, N., Chatila, T.A., and Gullberg, M. (1997). Regulation of microtubule dynamics by Ca2+/calmodulin-dependent kinase IV/Gr-dependent phosphorylation of oncoprotein 18. Mol. Cell. Biol. *17*, 3459–3467.

Ho, S.N., Hunt, H.D., Horton, R.M., Pullen, J.K., and Pease, L.R. (1989) Site-directed. mutagenesis by overlap extension using the polymerase chain reaction. Gene *77*, 51–59.

Horwitz, S.B., Shen, H.J., He, L.F., Dittmar, P., Neef, R., Chen, J.H., and Schubart, U.K. (1997). The microtubule-destabilizing activity of metablastin (p19) is controlled by phosphorylation. J. Biol. Chem. *272*, 8129–8132.

Howell, B., Deacon, H., and Cassimeris, L. (1999a) Decreasing oncoprotein 18/stathmin. levels reduces microtubule catastrophe and increases microtubule polymer in vivo. J. Cell. Sci. *112*, 3713–3722.

Howell, B., Larsson, N., Gullberg, M., and Cassimeris, L. (1999b). Dissociation of the tubulin-sequestering and microtubule catastrophe-promoting activities of oncoprotein 18/stathmin. Mol. Biol. Cell. *10*, 105–118.

Jourdain, L., Curmi, P., Sobel, A., Pantaloni, D., and Carlier, M.F. (1997) Stathmin. a tubulin-sequestering protein which forms a ternary T2S complex with two tubulin molecules. Biochemistry *36*, 10817–10821.

Koshland, Jr., D.E., Nemethy, G., and Filmer, D. (1966). Comparison of experimental binding data and theoretical models in proteins containing subunits. Biochemistry *5*, 365–385.

Larsson, N., Marklund, U., Gradin, H.M., Brattsand, G., and Gullberg, M. (1997). Control of microtubule dynamics by oncoprotein 18: Dissection of the regulatory role of multisite phosphorylation during mitosis. Mol. Cell. Biol. *17*, 5530–5539.

Larsson, N., Melander, H., Marklund, U., Osterman, O., and Gullberg, M. (1995). G2/M. transition requires multisite phosphorylation of oncoprotein 18 by two distinct protein kinase systems. J. Biol. Chem. *270*, 14175–14183.

Larsson, N., Segerman, B., Gradin, H.M., Wandzioch, E., Cassimeris, L., and Gullberg, M. (1999a). Mutations of oncoprotein 18/stathmin identify tubulin-directed regulatory activities distinct from tubulin association. Mol. Cell. Biol. *19*, 2242–2250.

Larsson, N., Segerman, B., Howell, B., Fridell, K., Cassimeris, L., and Gullberg, M. (1999b) Op18/stathmin. mediates multiple region-specific tubulin and microtubule-regulating activities. J. Cell. Biol. *146*, 1289–1302.

Lawler, S. (1998) Microtubule dynamics -. if you need a shrink try stathmin/op18. Curr. Biol. *8*, R212–R214.

Marklund, U., Brattsand, G., Shingler, V., and Gullberg, M. (1993) Serine 25 of oncoprotein 18 is a major cytosolic target for the mitogen-activated protein kinase. J. Biol. Chem. *268*, 15039–15047.

Marklund, U., Larsson, N., Gradin, H.M., Brattsand, G., and Gullberg, M. (1996) Oncoprotein 18 is a phosphorylation-responsive regulator of microtubule dynamics. EMBO J. *15*, 5290–5298.

Marklund, U., Osterman, O., Melander, H., Bergh, A., and Gullberg, M. (1994). The phenotype of a "Cdc2 kinase target site-deficient-"mutant of oncoprotein 18 reveals a role of this protein in cell cycle control. J. Biol. Chem. *269*, 30626–30635.

Ozon, S., Maucuer, A., and Sobel, A. (1997). The stathmin family – molecular and biological characterization of novel mammalian proteins expressed in the nervous system. Eur. J. Biochem. *248*, 794–806.

Walczak, C.E. (2000). Microtubule dynamics and tubulin interacting proteins. Curr. Opin. Cell. Biol. *12*, 52–56.